Fuel 325 (2022) 124784

Contents lists available at ScienceDirect

Fuel

journal homepage: www.elsevier.com/locate/fuel

Effect of process variables on producing biocoals by hydrothermal carbonisation of pine Kraft lignin at low temperatures

Umaru Musa [a,b], Miguel Castro-Díaz [a], Clement N. Uguna [a], Colin E. Snape [a,*]

[a] University of Nottingham, Faculty of Engineering, Energy Technologies Building, Triumph Road, Nottingham NG7 2TU, United Kingdom
[b] Department of Chemical Engineering, Federal University of Technology, P.M.B 65, Minna, Nigeria

ARTICLE INFO

Keywords:
Hydrothermal carbonisation
Pine Kraft lignin
Biocoal
Alkali and alkaline metals

ABSTRACT

Lignin from pulping is recovered in a wet form, making it ideal for hydrothermal carbonisation (HTC). This study investigates the effects of temperature (200–280 °C), residence time (1–6 h), and water to biomass mass ratio (2:1–6:1) on the composition of the resultant biocoal and the extent of alkaline and alkaline metal removal during HTC of pine Kraft lignin (PKL). Consistent with studies on other biomass materials, temperature exhibited the most significant effect on biocoal yield and properties, followed by residence time showing a marginal effect and varying the water to lignin mass only affecting alkaline and alkaline earth metals removal. Biocoal yields were in the range of 76–95 % (80–97 % on a carbon basis) and, compositionally, the biocoal obtained corresponded to sub-bituminous (220–260 °C) and high volatile bituminous coals (280 °C). Gas yields are low with the gas comprising mainly CO_2 (98 v/v). The optimum temperature, time and biomass to water ratio for alkaline and alkaline earth metals removal was 260 °C, 3 h and 5:1 under which 93–95 % for sodium (Na) and potassium (K) and 75–80 % for magnesium (Mg) and calcium (Ca) removal were achieved. Solid-state ^{13}C Nuclear Magnetic Resonance (NMR) revealed that during HTC, the oxygen-containing bonds of esters, ethers, and carboxylic groups were dissociated to produce lower-molecular weight including phenolic compounds dissolved in the process water. These findings have shown that the HTC is a promising alternative thermochemical route for coalification of wet PKL to a low ash coal-like fuel similar to sub-bituminous coal in rank that has potential applications for carbonisation.

1. Introduction

There is an increasing awareness of the challenges associated with the use of fossil fuels in the current energy consumption scheme because fossil fuel reserves are becoming depleted, and emissions from the burning of fossil fuels are contributors to climate change and global warming [1]. The Global Atmospheric Research emissions database revealed that the global CO_2 emissions arising from fossil fuel utilisation stand at approximately 36 Gigatonne in 2016 [2]. The United Nations (UN) Intergovernmental Panel on Climate Change (IPPC), reported that global CO_2 emissions need to be reduced by 45 % from 2010 levels by 2030 to limit the mean rise in global temperature to 1.5 °C by 2050 [3,4]. The use of biomass as a potential renewable, eco-friendly replacement for fossil fuels is widely acknowledged due to its carbon neutrality [4,5]. Biomass is the third-largest source of energy in the world after petroleum and coal [6]. Biomass can be converted into solid, liquid and gaseous fuels via different thermochemical conversion processes.

Hydrothermal carbonisation (HTC) is a relatively new thermochemical conversion process that combines both leaching and torrefaction in a single-step operation using water as a reaction medium. HTC is performed between 150 and 350 °C and 10–50 bar for a few hours (0.5–8 h) in an inert environment [7]. HTC is best suited for upgrading biomass feedstock containing high amounts of inorganic elements and moisture [8,9]. The main product of HTC is high yield (50–80 wt%), energy-dense, coal-like solid fuel (biocoal). The improvement in energy density is caused by the reduction in the hydrophilic functional groups through a decrease in hydrogen and oxygen contents [7,10,11]. Water is changed from a highly polar hydrogen-bonded substance to a non-polar organic solvent like hexane during the HTC [10]. This change in properties enables the subcritical water to provide a medium for several complex reactions such as hydrolysis, dehydration, and decarboxylation [12]. The HTC process results in the formation of liquid (bio-oil mixed with water), and minor proportion of gases (mainly CO2) in addition to

* Corresponding author.
E-mail address: colin.snape@nottingham.ac.uk (C.E. Snape).

https://doi.org/10.1016/j.fuel.2022.124784
Received 31 March 2022; Received in revised form 29 May 2022; Accepted 2 June 2022
Available online 16 June 2022

the solid product (hydrochar or biocoal). The percentage distribution and properties of the final products primarily depend upon the process operating conditions [13]. HTC biocoals are used as adsorbents, soil amender, supercapacitor electrodes, solid fuel [14] and nanostructured carbon catalysts [15]. HTC liquid products are rich in organic acids, and value-added platform chemicals [16]. The severity of HTC process conditions (residence time, temperature, and biomass-to-water) and difference in cellulose, hemicellulose and lignin composition of biomass are key factors that determine biocoal yield and quality. Biocoal yields are more from lignin than cellulose and hemicellulose and biomass [17–19].

Lignin is second only to cellulose in terms of quantity and availability [19,20]. It is the only renewable aromatic resource and makes up 20–35 % of biomass weight [21]. It contains various ether linkages, methoxy and hydroxyl groups, thus, highly oxygenated [22]. Lignin is obtained as a by-product in the pulping industry (mainly as Kraft lignin) and will be obtained as a waste product in future bio-refineries [23]. The Kraft process accounts for over 85 % (approximately 100 million dry tonnes) of the annual global production of lignin [23–26] and is projected to reach 225 million tonnes by 2030 [27]. Currently, nearly 98 % of available lignin is burned directly to generate energy [25,28]. The growing interest in the decarbonisation of industrial manufacturing processes has stimulated the urge to develop biocoals from lignin. Lignin has higher thermal stability and heating values than cellulose and hemicellulose [29,30]. Lignin atomic H/ C and O/ C ratios are closer to those of coal than parent biomass [17]. Thus, lignin is an attractive precursor for biocoal production due to its availability and high carbon content [28]. Most studies on hydrothermal treatment of lignin are limited to wet oxidation to produce aromatic aldehydes, liquefaction to produce phenolic oil or gasification to produce hydrogen and methane [15,20,29,31–34].

To date, few studies have investigated the HTC of lignin for biocoal production [28,31,35–42]. Nearly all these studies were limited to the effect of temperature on the structural evolution of lignin while the biocoals application was mostly focused on the activated carbon production. To the best of the authors' knowledge, a detailed systematic investigation of the combined influence of HTC time, temperature and lignin to water ratio on the physiochemical characterisation and extent of alkaline and alkaline earth metals removal from lignin with the view of producing a renewable alternative to coal is lacking in the literature. The satisfactory knowledge of the biocoal overall physicochemical properties and energy value as a function of temperature, time, and biomass-to-water ratio during carbonisation is also a prerequisite for the design of a functional HTC process [7–9]. These parameters are also known to influence the extent of biomass carbonisation and reactivity and need to be understood for biocoal [9,43]. According to Koppejan and Lo [44], the presence of these inorganics, (mainly Na and K), along with chlorine and sulphur in biomass influence ash chemistry and causes fouling, slagging and corrosion of combustion equipment. HTC reduces these ash related problems through the removal of a huge portion of these inorganics [45]. This is due to the increased ionic dissociation constant, decreased dielectric property and pH of the subcritical water which enhance the removal of ionic bonded inorganics through ion exchange and salts dissolution into the aqueous phase [8]. HTC has been proven to reduce inorganic metals content of corn stover, rice hull, switchgrass [46], Chinese fan palm [47], empty palm fruit bunches [48], softwood pellets and olive cake [9], miscanthus [45,49], and food waste [50]. However, there is no evidence of reported studies specific to extent of coalification and inorganic metals (alkaline and alkaline earth metals) removal of any type of lignin. Furthermore, no attention has been paid to the carbon yield and distribution during HTC of lignin.

To the best of our knowledge, the results presented in this study represent the first attempt to provide a better understanding of the changes in properties and energy content occurring within the pine Kraft lignin (PKL) under different HTC conditions (residence time, temperature, and biomass to water ratio). Thus, this paper (i) examines the influence of these HTC conditions on lignin biocoals synthesis as a suitable for coal; (ii) establishes the optimum conditions for the biocoal production iii); characterises the biocoal for its physicochemical characteristics, energy value, aromaticity, and extent of alkaline and alkaline earth metals removal.

2. Materials and methods

2.1. Materials

A pine Kraft lignin was obtained from MeadWestvaco (USA) and supplied as a dark brown powder (greater than 99.5 % lignin). Analytical grade Dichloromethane (99.8 %), hydrogen peroxide (30 %), nitric acid (65 %), and hydrofluoric acid (40 %) were purchased from Fisher scientific UK. Table 1 presents the characteristics of the PKL used.

2.2. Hydrothermal carbonisation

Hydrothermal carbonisation (HTC) was conducted in Parr 4740 series 75-ml stainless steel high-pressure autoclaves. Each experiment was conducted by measuring the known amount of PKL and deionised water in the reactor according to the conditions in Table 2.

The reactor was tightly capped, sealed, and a pressure gauge was attached. It was then flushed with nitrogen at a pressure of 1 bar to establish an inert atmosphere and then transferred into a fluidised sand bath and preheated to the desired temperature. The temperature was monitored using an additional K-type thermocouple connected externally to a computer that records the temperature every 10 s. The autoclave was heated up to the required temperature in a fluidised sand bath and the reaction is allowed to run for pre-determined conditions. After the reaction time was completed, the autoclaves were allowed to cool to room temperature. The liquid and solid fractions were collected, filtered, and the biocoal was washed with distilled water. The biocoals were dried in an oven set at 105 °C for at least 16 h and were labelled and kept for further characterization. The samples are labelled as Hxxx–y–z:w where xxx, y and z:w represent the HTC temperature residence time and biomass to water ratio respectively.

The mass and energy yield and carbon recoveries were calculated as:

$$\text{Biocoal (solid) yield (wt\%)} = \frac{\text{Biocoal weight}}{\text{Feedstock weight}} * 100 \quad (1)$$

$$\text{Gas yield (wt\%)} = \frac{\text{Mass of gas}}{\text{Feedstock mass}} * 100 \quad (2)$$

$$\text{Liquid yield (wt\%)} = 1 - (\text{solid yield} + \text{gas yield}) \quad (3)$$

$$\text{Energy yield (\%)} = \frac{\text{HHV Biocoal}}{\text{HHV feedstock}} * \text{Mass yield} \quad (4)$$

Table 1
Characteristics of the pine Kraft lignin (PKL).

Physicochemical properties	Value
Ash (wt%, db)	2.1
VM (wt%, db)	60.3
FC (wt%, db)	39.7
C (wt%, db)	62.3
H (wt%, db)	5.7
N (wt%, db)	0.8
S (wt%, db)	1.9
O* (wt%, db)	29.2
Ca (ppm)	178.6
K (ppm)	801.9
Mg (ppm)	170.7
Na (ppm)	7324.7
HHV (MJ/kg)	25.5

*By difference.

Table 2
Operational parameters for HTC.

Variables	Unit	Temperature					Time			Biomass to water mass ratio				
Temperature	°C	**200**	**220**	**240**	**260**	**280**		260				260		
time	h			1			**1**	**3**	**6**			3		
Biomass to water mass ratio				1:3				1:3		**1:2**	**1:3**	**1:4**	**1:5**	**1:6**

$$\text{Carbon recovery (wt\%)} = \frac{\text{Carbon in biocoal}}{\text{Carbon in feedstock}} * \text{Mass yield} \quad (5)$$

$$\text{Fuel ratio (FR)} = \frac{\text{Fixed carbon}}{\textit{Volatile matter}} \quad (6)$$

2.3. Proximate, ultimate composition and higher heating value

The proximate composition of samples was determined following the ISO562 and ISO 1171 standard procedures to obtain moisture (M), ash (A) and volatile matter (VM) determination. For ultimate analysis, the standard procedures ASTM D5016-98 and ASTM D5373-02 were used for the determination of C, H N and S using LECO CHN-2000 and LECO S-144DR instruments. The O content was determined by difference. The HHV were calculated from their elemental contents by the following equation (7) [51].

$$HHV = 0.3491C + 1.1783H + 0.1005S - 0.1034O - 0.0151N - 0.0211A \quad (7)$$

2.4. Inorganic elements analysis

Elemental concentration was determined following BS EN ISO 16967:2015. A CEM MARSX sealed vessel microwave digestion system was used for the total digestion. 50 mg of homogenized biocoal ash with 2 ml H_2O_2 (30 %), 3 ml HNO_3 (65 %), and 2 ml 40 % of hydrofluoric acid (HF) in a decomposition vessel and allow the solution to react for at least 5 min before sealing the vessel. The Agilent Technologies 5110 VDV Inductively coupled plasma optical emission spectroscopy (ICP-OES) instrument was used for the determination of elemental concentrations of the digested PKL, biocoals and process water collected after HTC. The minerals measured were Na, Ca, Mg and K.

2.5. Solid-state ^{13}C nuclear magnetic resonance (NMR)

Cross polarization (CP) coupled with magic angle spinning (MAS) solid-state ^{13}C nuclear magnetic resonance (NMR) analyses were performed with a Bruker Avance 200 spectrometer at a field strength of 4.7 T. The field strength corresponds to resonance frequencies of 50 MHz for ^{13}C and 200 MHz for 1 h. The samples were packed tightly into a zirconia rotor with a Kel-F rotor cap and spun at the magic angle (54° 44′) with a spinning frequency of approximately 5 kHz. A contact time of 1 ms was used during the Hartmann-Hahn condition. The acquisition time was 1.5 s and the spectra were obtained after 2500 scans. The free induction decay (FID) was processed using a line broadening factor of 50 Hz. Tetrakis (trimethylsilyl) silane (TKS) was used as a standard for calibrating the sample peak's position.

2.6. Gas analysis

Gas collected into an airtight bag was immediately analysed using Clarus 580 gas chromatograph (GC) fitted with a Flame ionization detector (FID) and thermal conductivity detector (TCD) detectors operating at 200 °C. The hydrocarbon gases were analysed by injecting 100 µl of gas samples (split ratio 10:1) onto the FID at 250 °C with separation performed on an alumina plot fused silica 30 m × 0.32 mm × 10 µm column, with helium as the carrier gas. The oven temperature was programmed from 60 °C (13 min hold) to 180 °C (10 min hold) at 10 °C min^{-1}. Individual hydrocarbon gas yields were identified and quantified using C_1-C_5 gases (injected separately) as an external gas standard. The non-hydrocarbon gases (H_2, CO and CO_2) were analysed by injecting 500 µl onto the TCD. Separation was performed on a Haysep N6 packed column using Argon as the carrier gas. The oven temperature was programmed from 60 °C (13 min hold) to 160 °C (2 min hold) at 10 °C min^{-1}.

2.7. Gas chromatography-mass spectrometry (GC–MS) analysis of the liquid products

The analysis of the dichloromethane-extracted liquid phase was performed using an Agilent GC–MS (7890B GC; 5977A MSD), with a single quadrupole mass spectrometer and an electron impact ionization detector (EID). The GC injector was kept at 280 °C, and the injection split ratio and the injection volume were 10:1 and 1 µl, respectively. The organic phase products were separated with a DB-1701 MS column (60 m × 0.25 mm i.d. × 0.5 µm film thickness, Agilent Technologies, Inc., USA). The temperature ramp of the GC column oven began with a constant temperature step at 50 °C for 2 min and then increased by a rate of 4 °C/min up to a final temperature of 280 °C which was held constant for 20 min. Helium (99.99 % purity) was used as a carrier gas with a 1.2 ml/min volume flow. The MS ionization mode was electron impact at 70 eV and the mass scan range was from 29 to 450 *m/z*. The various liquid phase products were identified by comparing all chromatogram spectra to the National Institute of Standards and Technology (NIST) mass spectral search program and the Wiley mass spectrum library. Measurements were conducted in triplicate for all the HTC and characterization techniques, and a mean value was reported. The error margin associated with all the analyses was within ± 1.5 %.

3. Results and discussion

3.1. Mass and carbon yields

Fig. 1a presents the biocoal yield as a function of temperature (200 °C–280 °C) using biomass to water mass ratio of 1:3 and residence time of 1 h. HTC at lower temperatures (200–240 °C) showed a less significant effect on both the dry, ash-free biocoal mass yield because these temperatures were not sufficient to facilitate the decomposition of the major components of the PKL thereby resulting in higher biocoal yield (88–90 wt%). The biocoals obtained at these temperatures were only partially carbonised, displaying a brownish colour similar to the PKL. The high yields obtained under these conditions indicate that less than *ca.* 12 wt% of lignin was converted into gaseous and liquid products (including water) at temperatures below 250 °C. The subsequent, increase in HTC temperature from 240 to 280 °C results in a steady decline in biocoal mass yield from 88 to 76 wt% and a corresponding increase in gaseous and liquid products respectively. The biocoal yield obtained at this higher temperature was visibly transformed into a homogenous blackish coal-like fuel.

Similarly, Fig. 1b shows that the mass yield of biocoal also decreased from 83 to 76 wt% as residence time increased from 1 to 6 h at 260 °C using biomass to water ratio of 1:3. This was followed by a simultaneous increase in gas and liquid yield from 4 and 13 wt% to 5 and 19 wt% respectively. The increase in the amount of gas and liquid produced at longer residence times could be explained by the degradation of soluble lignin fragments in the aqueous phase. The lower yield of biocoal

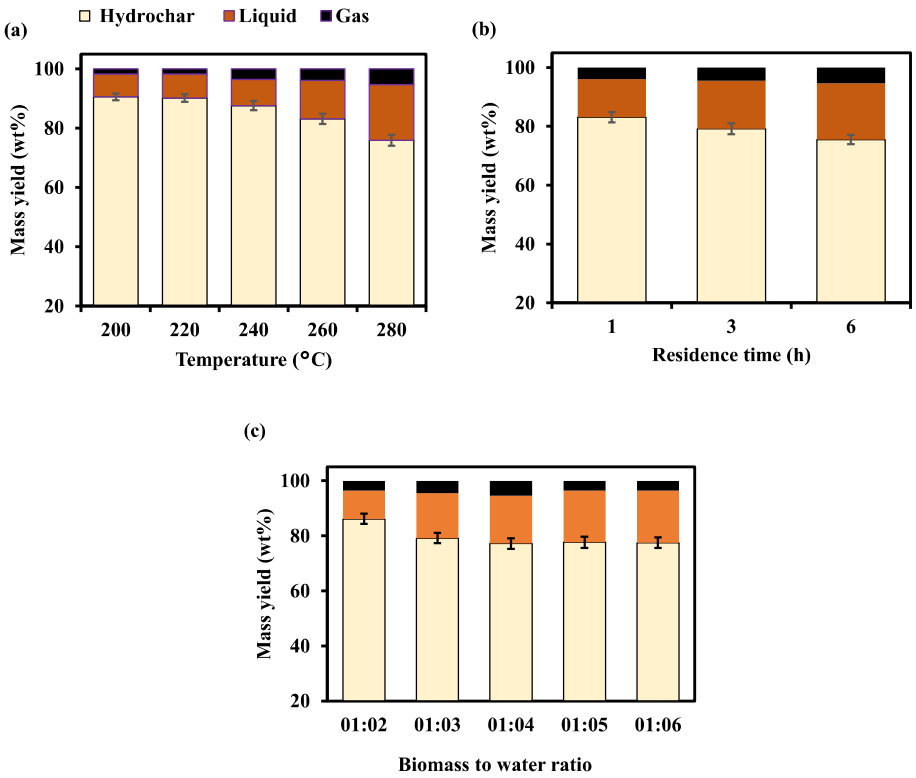

Fig. 1. Biocoal mass yield as a function of (a) temperature at a residence time of 1 h and biomass to water mass ratio of 1:3 (b) different residence time at temperature of 260 °C and water to biomass mass ratio of 1:3 (c) different water to biomass ratio at a temperature of 260 °C and residence time of 3 h.

obtained at higher temperature and longer residence time signifies that hydrolysis, decarboxylation and dehydration reactions were more favourable under these conditions. The mass yield of 79–90 wt% observed in this study was consistent with 76 and 88 wt% reportedly obtained from HTC of organosolv and Klason and lignin by Kang et al. [52] and Atta-Obeng et al. [42] respectively.

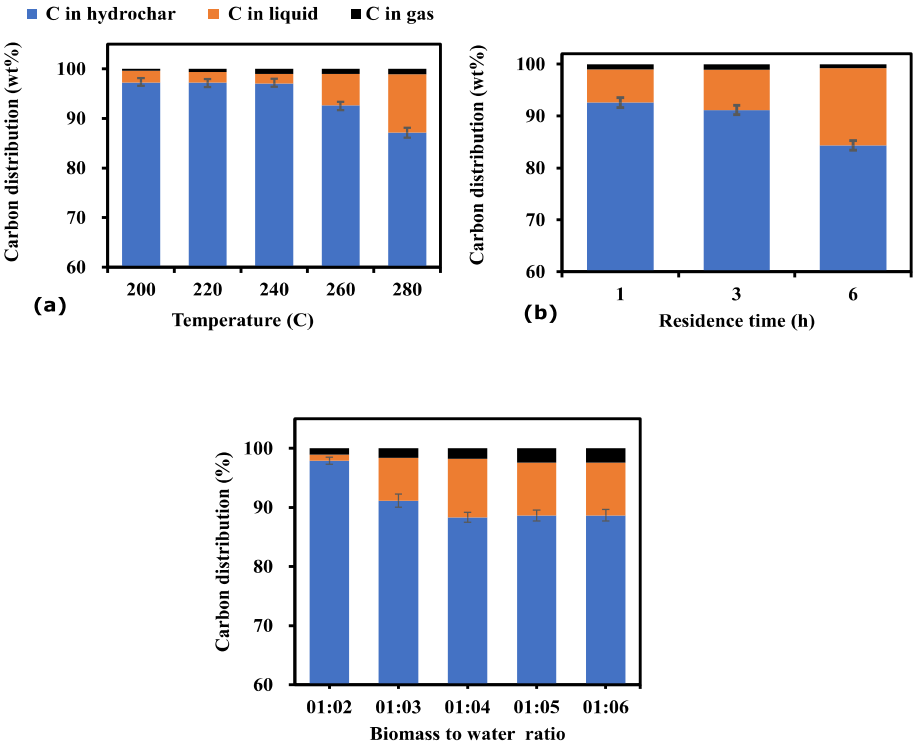

Fig. 2. Carbon distribution in biocoal, liquid and gaseous products as a function of (a) temperature at a residence time of 1 h and biomass to water mass ratio of 1:3 (b) different residence time at a temperature of 260 °C and biomass to water mass ratio of 1:3 (c) different water to biomass ratio at a temperature of 260 °C and residence time of 3 h.

Water acts as a reactant, catalyst and solvent that aids the hydrolysis and decomposition of biomass during HTC [7]. The effects of different biomass to water mass ratios in Fig. 2c show that low water concentration (1:2) does not promote the rapid degradation of PKL probably due to the insufficiency in the amount of water compared to the amount of PKL. Thus, it can be deduced that increasing the biomass-water ratio further from 1:2 to within a range of 1:3–1:4 drives the reaction faster to equilibrium thereby promoting faster degradation of the organic waste within the feedstock and enhancing gaseous and liquid product formation. This was evident by the increase in the liquid product yield from 10.3 wt% at a ratio of 1:2 to about 18 wt% at a ratio of 1:4 and an even higher ratio. The biocoal mass yield noticeably decreases from 86 wt% at 1:2 to approximately 79 wt% at 1:3 thereafter remaining nearly the same (~ 78 wt%) with a further increase in ratio from 1:3 to 1:6 ratio.

The carbon distribution within the biocoal, liquid and gaseous phases produced from HTC of PKL across varying temperature, residence time and biomass to water ratios presented in Fig. 3 follow similar trends as the mass yield.

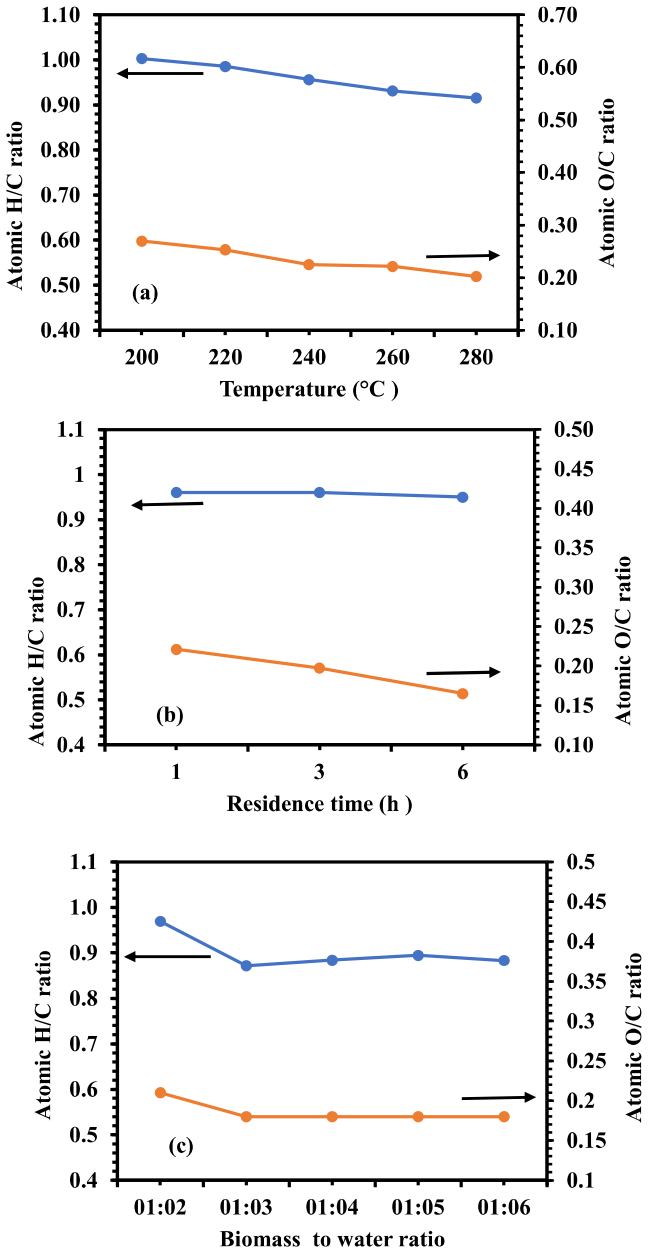

Fig. 3. The effect of (a) temperature on the atomic H/C and O/C ratios with biomass to water mass ratio of 1:3 and a time of 1 h (b) residence time at a temperature of 260 °C with biomass to water mass ratio of 1:3 (c) biomass to water mass ratio at a temperature of 260 °C and residence time of 3 h.

Fig. 2a shows that an increase in temperature results in a progressive decline in the biocoal carbon yield to 75.89 wt% of the C content of the initial PKL, while the carbon content of gas and liquid phases increases correspondingly. The reduction in carbon yield with increasing HTC temperature can be attributed to greater solubilisation and diffusion of carbon into the liquid and gas phases. At 200 °C, only approximately 0.4 and 1.1 % of the initially present carbon were transferred to the gas and liquid phase respectively, as against 2.4 % and 11.6 w% of carbon as the temperature rises to 280 °C for the same residence time (1 h). The reduction in carbon yield with an increase in temperature observed in the study was consistent with the trend reported by Hoekman et al. [53] and Atta Obeng et al. [42] respectively.

The biocoal carbon yield also decreases to 93, 91 and 84 wt% as HTC residence time increases to 1, 3 and 6 h, respectively. This was followed by a slight increase in liquid (8 wt%) and gases (1 wt%) after 3 h. The subsequent increase in residence time to 6 h resulted in 15 and 0. 8 wt% of carbon to the liquid and gaseous phases, respectively (Fig. 2b). In the case of biomass to water mass ratio, the fraction of carbon retained in biocoal only decreased pronouncedly from 98 to 88 wt% as the biomass to water mass ratio was increased from 1:2 to 1:4 and thereafter remain nearly constant with further increase ratio. These findings revealed that a significant proportion of carbon was retained within the biocoal after HTC under these conditions (Fig. 3c). The high carbon yield (> 85 wt%) obtained in this study suggests that carbon recovery from HTC of lignin is comparatively higher than thermochemical conversion methods [54].

The relative proportion of gaseous products measured by GC analysis under different HTC conditions is presented in Table 3. Gas yields increase with increasing temperature and time but remain unchanged beyond the biomass to water mass ratio of 1:3. CO_2 was found to be the most dominant gas produced accounting for 97 % (vol.) under all conditions. The CO_2 yields increase from 5.5 mg/g at 200 °C to 24.2 mg/g at 280 °C. The variation of residence time from 1 to 6 h at 260 °C results in a corresponding increase in CO_2 yield from 17 mg/g to 29 mg/g. No significant increase was observed as the biomass to water ratio was increased from 1:2 (17 mg/g) to 1: 6 (19 mg/g). The high proportions of CO_2 observed in this study are consistent with literature reports [30].

The formation of CO_2 and CO primarily originates from decarboxylation and decarbonylation. According to Funke and Ziegler [12], a higher HTC temperature greater than 150 °C eliminates the carboxyl (–COOH) and carbonyl (C═O) groups via decarboxylation to give off CO_2

Table 3
Gas composition at different temperatures, residence times and biomass to water ratio.

Gases	CH_4	C_2–C_5	H_2	CO	CO_2	Total
Temperature	(mg/g)					
H200-1-1:3	<0.01	<0.01	<0.01	0.02	5.45	5.47
H220-1-1:3	0.01	<0.01	<0.01	0.09	7.90	7.99
H240-1-1:3	0.02	0.02	<0.01	0.11	15.84	15.99
H260-1-1:3	0.05	0.04	<0.01	0.30	16.56	16.96
H280-1-1:3	0.06	0.07	<0.01	0.64	24.17	24.95
Time						
H260-1-1:3	0.05	0.04	<0.01	0.30	16.56	16.96
H260-3-1:3	0.09	0.07	<0.01	0.45	22.75	23.36
H260-6-1:3	0.12	0.10	<0.01	0.19	28.86	29.26
Biomass to water mass ratio						
H260-3-1:2	0.06	0.24	<0.01	0.20	17.05	17.55
H260-3-1:3	0.09	0.07	<0.01	0.45	22.56	23.17
H260-3-1:4	0.07	0.89	<0.01	0.45	21.77	23.18
H260-3-1:5	0.30	0.55	<0.01	0.59	21.39	22.83
H260-3-1:6	0.46	0.49	<0.01	0.45	19.05	21.45

and CO as gases. Other gases produced include small amounts of hydrocarbon gases (methane, ethane, ethene, propene, propane, butane, butene, pentane) and minor traces of H_2.

3.2. Ultimate and proximate composition

The ultimate analysis of the raw PKL and biocoals are presented in Table 4. The results show that an increase in temperature and residence time increases the biocoal carbon content by 10–15 wt%, corresponding to reductions in oxygen and hydrogen contents. The carbon content increased appreciably with an increase in the severity of temperature and time, to obtain a maximum of 73 wt% and 76 wt% respectively (Table 4).

No significant change in carbon content was observed beyond biomass to water mass ratio of 1:3. The oxygen of the samples decreased with an increase in temperature and time and varies between 17 and 22 wt%. It is important to highlight that the carbon content of biocoal obtained in this study was high (67–75.9 wt%). The higher carbon of a biocoal the higher the energy contents [55]. As regards the nitrogen and sulphur content, the nitrogen remains nearly unaffected by HTC treatment but only changes negligibly. This observation was consistent with the previous finding on the hydroprocessing of lignin [52]. The sulphur content decreases from 2 to approximately 1 wt% with temperature increase but remains the same with change in residence time from 1 to 6 h and was not affected by the change in biomass to water ratio. This can be attributed to the fact that sulphur exists in lignin as sulfide, sulfate ions, and organically bound sulphur [56].

The proximate analyses of the pine Kraft lignin and biocoals are presented in Table 2 summarizes that the increase in HTC temperature and residence time causes a decrease in the volatile matter fragments and increases fixed carbon in the biocoal. Regarding the effect of temperature, the lowest volatile matter (48. wt%) is obtained for the sample H280–1–1:3, indicating a 27.7 % reduction. A similar trend was observed for residence time variation where the maximum volatile reduction (44.7 wt%) was obtained for the H280–6–1:3 sample, which represents a decrease of 33.3 % and a corresponding increase in fixed carbon to 55 wt%. This appreciable reduction in the VM content was attributed to the devolatilization that occurs during the HTC process. Lower volatile matter and increased fixed carbon content of biocoals are associated with reduced emission of gases and improved biocoal combustion efficiency [57]. Thus, biocoal has the potential to produce a more stable flame with reduced combustion speed. In the case of variation of biomass to water ratio, the change in this parameter does not affect the proximate composition. The ash content of the lignin was low and decreases from 2.1 wt% in the raw PKL to 1.0 wt% as HTC temperature increased from 200 to 280 °C (Table 2). All the biocoals contain less ash (0.65–1.09 wt%) than the raw PKL (2.1 wt%) corresponding to a decrease of about 52–70 % compared to the ash content of the raw PKL. Lower ash content helps to minimize slagging and soot formation. The ash value observed in this study was lower than those reported for both brown and black coals [58–62] and a wide range of biocoals produced from different lignocellulosic biomass feedstocks, which were between 5 and 31 wt% [63]. The low ash contents observed in this study were similar to those reported for biocoals produced from other lignin samples [28,52]. The fuel ratio (FR) of biocoal increased from 0.88 to 1.02 as HTC the temperature increased 200 to 280 °C and 1.02 to 1.24 as the residence time increased from 1 to 6 h respectively as against 049 for raw PKL. Importantly, the FR for the sample H260–6 h–1:3 was almost three times greater for the initial PKL. The improvement in the biocoal FR with temperature and time is attributed to the reduction in biocoal VM content and increase in the FC content as presented in Table 4. Biomass to water does not show any effect on the FR. However, the highest biomass to water ratio of 1:6 is associated with a slight decrease in the FC of biocoal.

3.3. Energetic properties of biocoal samples

The analysis of biocoal energetic properties is presented in Table 5. The energy densification ratio (EDR) is defined as the ratio of higher heating value (HHV) of the biocoal to feedstock. The calculated HHV and energy densification factor were found to increase with increasing carbonization temperature and time. The values obtained in this study lie within the ranges of 28–32 MJ/kg and 1.07–1.20, respectively (Table 5). The substantial improvement in HHV was attributed to the degradation of low-energy chemical bonds and the generation of high-energy chemical bonds, respectively [11]. HHV increases significantly with temperatures increase, mildly with an increase in residence time and with no observable change with increasing biomass to water mass ratio. The HHV (20–30 MJ/kg) obtained in this study was very consistent with the American coal classification standard (27.56–30.89 MJ/kg) for medium and high volatile matter bituminous coals [64]. The increase in HHV is accompanied by a decrease in energy yield (ratio of energy content in the biocoal to the energy content of precursor).

However, the energy yield of 87–98 % obtained was far greater than

Table 4
Ultimate, proximate and fuel properties of pine Kraft lignin biocoals were obtained at different temperatures for a residence time of 1 h and biomass to water mass ratio of 1:3. Data for the PKL are also shown for comparison purposes.

Properties	C	H	N	S	O*	A	VM	FC	FR
Variables	(wt%, db)						(wt%, daf)		
Temperatures									
PKL	61.1	6.3	0.8	1.9	27.8	2.1	67	33	0.49
H200-1-1:3	67	5.6	0.6	1.3	24.1	1.4	53.2	46.8	0.88
H220-1-1:3	68.2	5.6	0.6	1.21	22.99	1.4	51.6	48.4	0.94
H240-1-1:3	70.3	5.6	0.7	0.98	21.07	1.35	50.9	49.1	0.96
H260-1-1:3	70.9	5.5	0.6	0.98	20.92	1.0	49.4	50.6	1.02
H280-1-1:3	72.1	5.5	0.7	0.97	19.43	1.3	48.4	51.6	1.07
Time									
H260-1-1:3	70.9	5.5	0.6	0.98	20.92	1.1	49.4	50.6	1.02
H260-3-1:3	73.1	5.31	0.7	0.95	19.24	0.7	46.4	53.6	1.16
H260-6-1:3	75.6	5.22	0.7	0.94	16.64	0.9	44.7	55.3	1.24
Biomass to water ratio									
H260-3-1:2	71.8	5.8	0.8	0.97	19.18	1.45	46.3	53.7	1.16
H260-3-1:3	73.1	5.31	0.7	0.95	18.33	1.61	46.4	53.6	1.16
H260-3-1:4	73.3	5.4	0.8	0.94	18.32	1.24	46.5	53.5	1.15
H260-3-1:5	73.1	5.51	0.8	0.96	18.98	0.65	46.3	53.7	1.16
H260-3-1:6	73.5	5.41	0.8	0.97	18.23	1.09	47.2	52.8	1.12

Table 5
Fuel properties of pine Kraft lignin and biocoal samples obtained at different HTC conditions.

Samples ID	HHV (MJ/kg)	EDR	EY (%)	H/C	O/C	Ar
Temperature						
PKL	25.5	1.00	100	1.24	0.34	0.67
H200 – 1 h – 1:3	27.59	1.06	96.02	1.00	0.27	0.70
H220 – 1 h – 1:3	28.11	1.08	97.43	0.99	0.25	0.70
H240 – 1 h – 1:3	29.02	1.12	97.74	0.96	0.22	0.72
H260 – 1 h – 1:3	29.13	1.12	93.08	0.93	0.22	0.75
H280 – 1 h – 1:3	29.70	1.14	86.60	0.88	0.16	0.77
Time						
H260 – 1 h – 1:3	29.13	1.12	93.08	0.93	0.22	0.75
H260 – 3 h – 1:3	29.86	1.15	90.86	0.87	0.20	0.75
H260 – 6 h – 1:3	30.89	1.19	89.66	0.83	0.17	0.76
Biomass to water ratio						
H260 – 3 h – 1:2	29.97	1.15	98.09	0.97	0.20	0.74
H260 – 3 h – 1:3	29.93	1.15	91.08	0.87	0.19	0.75
H260 – 3 h – 1:4	30.11	1.16	89.33	0.88	0.19	0.76
H260 – 3 h – 1:5	30.12	1.16	89.93	0.88	0.19	0.75
H260 – 3 h – 1:6	30.21	1.16	90.01	0.88	0.19	0.74

Ar - Aromaticity.

the 26–30 % reported for anaerobically digested press cake derived biocoal [8], 74 and 86 % for dry manure and Japanese larch derived biocoal [65] and 62 % for cellulose derived biocoal [66] respectively.

3.4. *Effects of hydrothermal parameters on the extent of coalification*

The degree of coalification can be evaluated using the H/C and O/C atomic ratios presented in Table 5. The atomic H/C and O/C ratios of the biocoal samples in the range of 0.85–1.0 and 0.18–0.27, respectively were lower than 1.24 and 0.34 for the raw PKL sample (Table 5). Fig. 4a shows that increasing HTC temperature within the range of 200–280 °C results in a reduction of the biocoal atomic H/C and O/C ratios. The increase in residence time from 1 to 6 h had a similar but lesser effect than HTC temperature (Fig. 4b). The biomass to water mass ratio variation did not have any significant effect on the atomic ratio beyond 1.3 (Fig. 4c). The reduction in atomic ratios with change in HTC process conditions is attributed to the loss of hydrogen and oxygen atoms through the dehydration and decarboxylation reactions and the corresponding increase in carbon content via carbonization reactions. Generally, the lower atomic H/C and O/C ratios suggests higher aromaticity and lower polarity of biocoal, respectively. According to Leng et al [67], a higher degree of aromatic condensation implies enhanced biocoal stability. This suggests that the resultant biocoals will possess higher resistance to microbial and thermal degradation. The decrease in atomic H/C and O/C atomic ratios could be explained by the decomposition of functional groups mainly including acidic (carboxyl); basic (chromene, ketone, pyrone, and quinone) and alkyl (CH_3 and CH_2) groups [68]. The degradation of some of these biocoal surface functional groups results in the formation of a high amount of CO_2, and CO, and insignificant CH_4 and H_2 as evident in Table 3.

The degree of coalification of organic material to produce a carbon-rich material can also be presented using a van Krevelen diagram as shown in Fig. 4. This diagram serves as an index for quantifying the coal band of organic matter [69] and the maturation tendency of biomass to coal-like material.

It is visibly clear from Fig. 4 that the raw precursor (lignin) transforms into a coal-like material with variation in process conditions. The H/C and O/C atomic ratios drop from 1.24 and 0.34 for raw PKL to 0.88 and 0.16, respectively thereby causing the coalification band to shift from the biomass region towards the coal region at the bottom left as the severity of HTC (higher temperatures or longer times) increases. This is substantiated by the earlier decrease in oxygen content observed in Table 4. The value of the H:/C and O/ C ratios in this study was lower

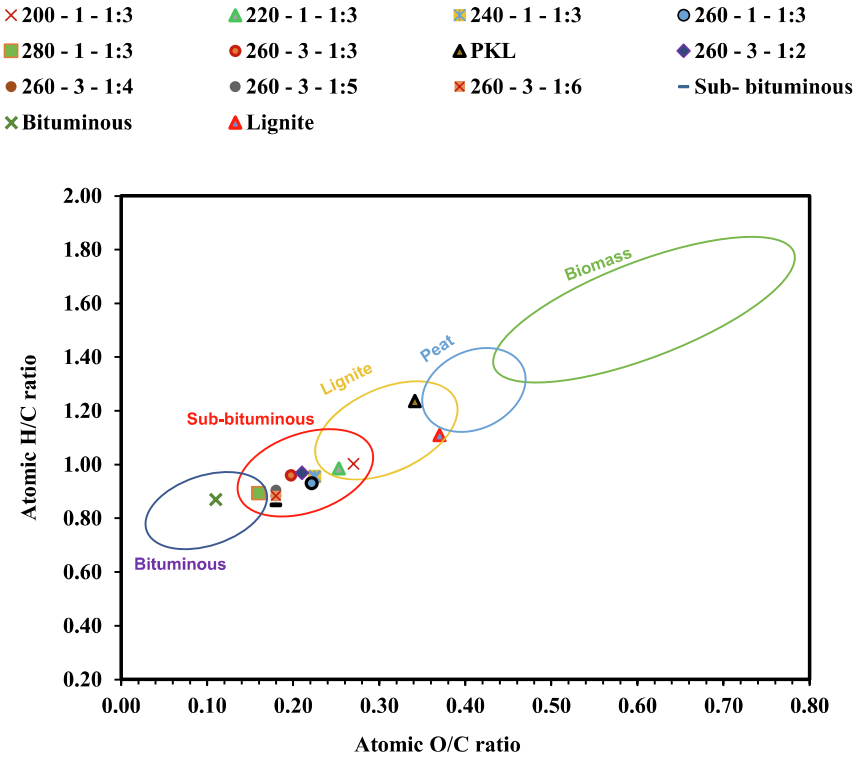

Fig. 4. Van Krevelen diagram of elemental atomic ratios for PKL and biocoals produced under different hydrothermal conditions.

than that of the same pine Kraft lignin after torrefaction [58] and lignite (1.11, 0.37) but overlaps bituminous (0.74–0.88, 0.10–0.11) and sub-bituminous coals (0.85, 0.18) [70,71] in the van Krevelen diagram (Fig. 4).

3.5. Effects of hydrothermal parameters on alkaline and alkaline earth metals removal

The presence of these metals has a marked effect on the ash chemistry, slagging behaviour, and fouling tendency of the biomass fuel which might cause boiler/furnace corrosion [72]. Fig. 5a shows that the extent of alkaline metals (Na, K) removal from the biocoal increases with temperature with over 82 % removal respectively at 260 °C as against 73 % at 200 °C. The further increase in HTC temperature up to 280 °C decreased the extent of alkaline metal removal with lower biocoal yield. Regarding the alkaline earth metals (Ca and Mg) removal, the Ca removal rate increases progressively to a maximum of 56.71 % as HTC temperature increase up to 260 °C. However, with further increase in temperatures, less calcium was removed while the Mg removal rate increases up to about 56.62 % at same temperature after which no significant removal was observed.

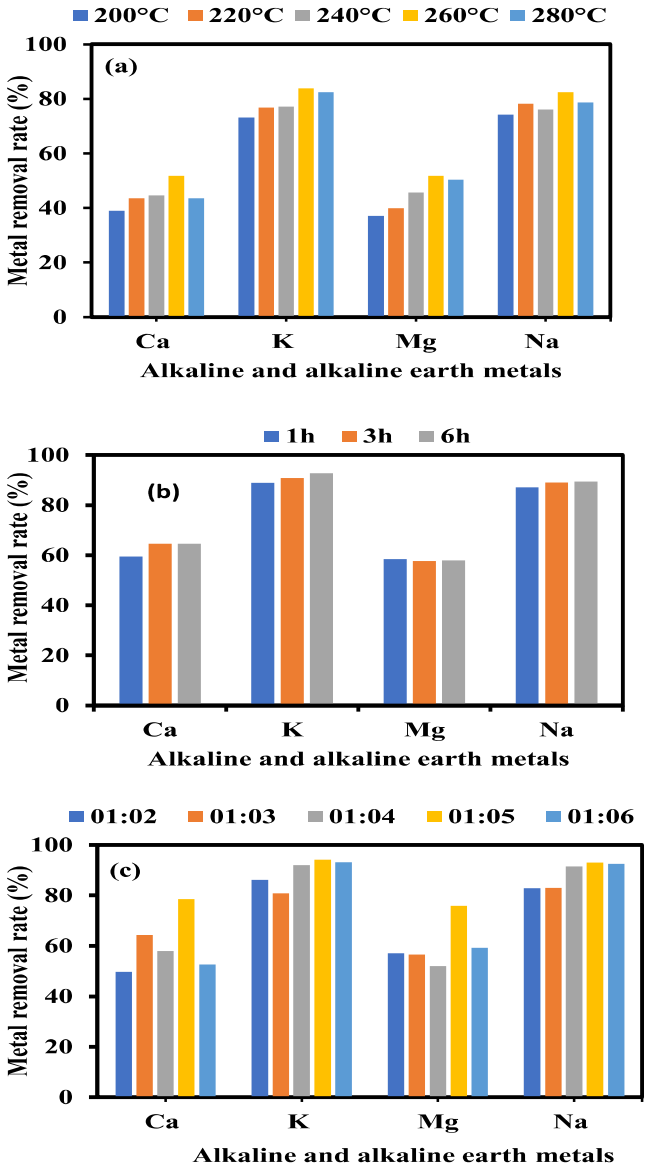

Fig. 5. Alkaline and alkaline earth metals removal rate (%) as a function of (a) temperature at a residence time of 1 h and biomass to water mass ratio of 1:3 (b) different residence time at a temperature of 260 °C and biomass to water mass ratio of 1:3 (c) different water to biomass ratio at a temperature of 260 °C and residence time of 3 h.

This observation signifies that significant amount of metals (especially Ca and Mg) were still retained within the biocoal at higher HTC temperatures. A possible explanation for a reduction in the rate of the metal at higher temperature might be due to the increased surface functionality and porosity of the biocoals at a high temperature which enables it to retain these divalent cations metals via ion exchange after adsorption from process water [7,8]. Chen et al. [73] also stated that Ca and Mg metals play a significant role in biocoal formation by acting as nuclei around which the char could be formed. These findings bear resemblance with the observation of Smith et al. [8] and Su et al. [50] during HTC of different lignocellulose biomass samples.

Fig. 5b shows that the removal rate of alkaline (Na and K) and alkaline earth metals (Mg and Ca) also increases with increasing residence time. As residence time increased from 1 h to 6 h, the removal rate of Na, K, Ca and Mg were 90 %, 92 %, 65 %, and 58 %, respectively. These results indicated that longer residence time enhanced the rate of removal of these metals. Regarding, the effect of biomass to water mass ratio shown in Fig. 5c the rate of metal removal increases with increasing biomass to water ratio until a ratio of 1:5 where optimum removal was attained. The maximum removal rate was in the order of K (95 %) > Na (93 %) > Ca (75 %) > Mg (73 %) respectively.

The observation in this study implies that Ca and Mg were less extracted than the alkaline metals. The percentage removal of the metals is in the order of Ca < Mg < K < Na. According to Smith et al. [8], the high removal efficiency of Na and K can be due to the existence of a high percentage of these metals in the form of soluble ionic salts within the biomass, making them possess a higher affinity with the liquid phase at elevated conditions [74,75]. The lower extent of removal of calcium and magnesium is due to the metal's association with organic matter in the biomass [8].

3.6. Solid-state ^{13}C NMR solid-state analysis

The ^{13}C CP/MAS NMR spectra were acquired for the PKL and biocoal char samples and the results are presented in Fig. 6. The assignment chemical shift was according to previous literature [28,76,77]. The internal standard (TKS) shows a peak at 3.5 ppm in the spectrum. Fig. 6a compares spectra of PKL and biocoal produced after HTC at different temperatures. The signals observed at 10–50 ppm correspond to aliphatic carbons (C—C), at 70–90 ppm (polysaccharides and aliphatic C—O carbons) and lignin propyl side chains.

The large peak at around 56 ppm originates from oxygenated alkyl carbons, such as methoxy groups (CH_3O –), alkyl-O-aryl ether (i.e., b-O-4, a-O-4) in the lignin structures while the broad peak between 145 and 148 ppm corresponds to aromatic carbon structure bonded to methoxyl groups (Ar–OCH_3) such as guaiacyl and syringyl units [28,76]. The absence of peak signals between 90 and 102 ppm indicates minute or no carbohydrates in the samples [78]. The presence of carbonyl (C═O) and carboxyl (– COOH) functional groups was also observed at 180 ppm for PKL. The aromatic peaks (C═C) can also be found between 120 and 127 ppm. Fig. 6b shows that the relative intensity of aliphatic carbon peaks at 10–50 ppm and oxygenated aliphatic carbons including methoxyl groups at 57 ppm and 145–148 ppm, respectively are similar for biocoal samples obtained at 200 and 240 °C while a sharp reduction occurs as temperatures increase to 240 and 280 °C. Similarly, the variation of HTC residence time from 1 to 6 h indicates that an increase in HTC residence time causes similar structural modifications in PKL as there is a slight reduction in aliphatic carbon. These small reductions in aliphatic and carbonyl carbon spectra suggest that HTC residence time has less effect on the aromatic structure evolution of the biocoals in comparison to temperature. This observation was consistent with the carbon content reported earlier where a minor increase in carbon content was observed

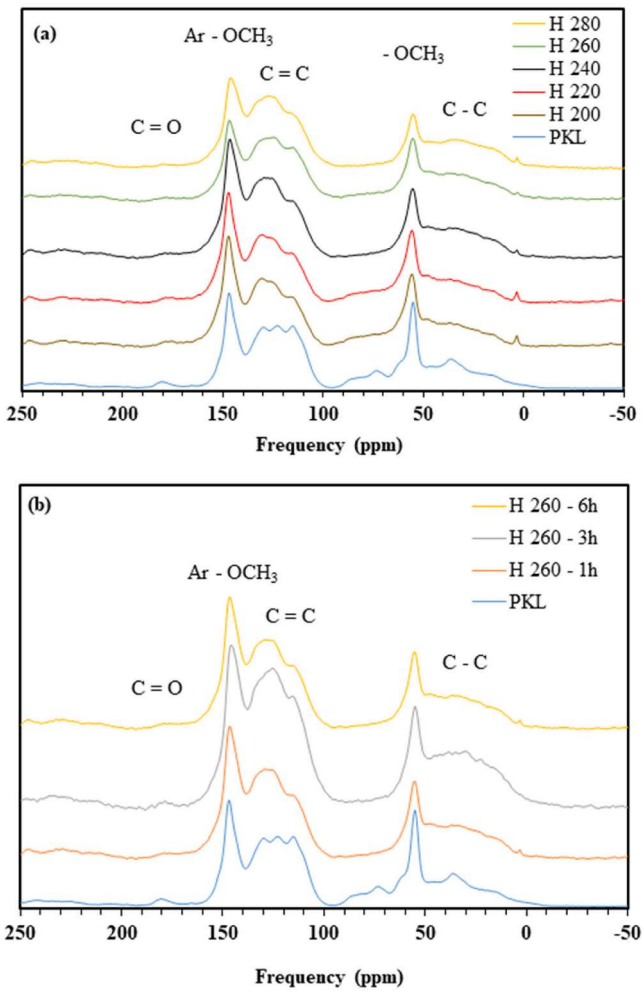

Fig. 6. Solid-state CP/MAS ^{13}C NMR spectra of (a) pine Kraft lignin were obtained at different temperatures with at a residence time of 1 h and (b) at different residence times at a temperature of 260 °C, at a water to biomass mass ratio of 3:1.

with increases in residence time. The relative intensity of the aromatic carbon (C═C) peak at 120–127 ppm was observed to increase in comparison with the PKL. The peak intensity increase within this region was attributed to decarboxylation, dehydration and enhanced polymerization reactions [79]. This indicates that higher temperatures and longer residence time cause greater degradation of the propyl side chain and methoxyl substituents of the aromatic ring which occur due to the cleavage of the unstable ether bonds within the PKL. On the other hand, the variation of biomass to water ratio from 1:2 to 1.6 has no significant change in the carbon structure. Thus, all the spectrum of various ratios bears similarity to spectra obtained for HTC 260–3 h in Fig. 6. The increase in aromatic carbon with increasing temperatures and time reported here was consistent with the earlier studies of Atta - Obeng et al. [42].

The aromaticity (Ar) is the ratio of aromatic carbon to the total carbon in the sample. Table 5 shows that the aromaticity of the initial PKL (0.67) increases progressively to 0.70 for biocoal produced at 200 °C, and further to 0.77 for the 280 °C biocoal, demonstrating that the biocoal degree of aromatization is directly proportional to HTC temperature. The aromaticity of the biocoals was however found to be inversely proportional to the oxygen content reduction with a coefficient of determination (R^2) of 0.98. The aromaticity (0.70–0.77) reported in this study was lower than ≥ 0.85 reported for good coking coal [80]. It was however higher than the aromaticity of lignite (0.45), subbituminous coal (0.65) and consistent with the aromaticity of 0.72 and 0.73 reported for low volatile matter bituminous (0.72), high volatile matter bituminous (0.73) coals [81], and medium volatile matter bituminous (0.75–0.77) [80].

3.7. GC–MS identification of lignin-derived monomers in the liquid products

Table 6 lists the products identified and their retention time of the dichloromethane-soluble portion of the liquid product after HTC of PKL at different conditions. The phenolic monomers identified can be categorised into three namely: G-type monomers, S-type monomers and polyphenols (PP) type monomers respectively. The G-type monomers having guaiacyl nuclei (2-methoxy phenol) as the parent building block make up a relatively high proportion (60–97 %) of the liquid products. Typical of these monomers present in the dichloromethane-soluble portion of the HTC liquid is 2-methoxy- Phenol (Guaiacol), 2-methoxy-3-methyl- Phenol, 4-ethyl-2-methoxy Phenol, 2-methoxy-4-propyl- phenol, vanillin, apocynin, Vanillyl methyl ketone, homovanillyl alcohol, 1-(2-Hydroxy-4-methoxyphenyl) propan-1-one, butyrovanillone, coniferyl alcohol, 4-(3-hydroxy-2-methoxyphenyl)-Butan-2-one, guaiacol propanol. Syringol (2,6 dimethoxy-4-propyl- phenol) is the only compound identified for the S-type monomers and it accounts for 1.2–2.7 % of the total phenolics. The contents of PP monomers in the liquid products are relatively small (1.7–33 %) compared to the G-type. The identified monomers include phenol, m-cresol, O-cresol, p-cresol, 4-ethyl- phenol, catechol and 3,4-dimethoxy-phenol. A similarly high proportion of G-type monomers with variation in product distribution were reported in previous studies [30,82,83]. The difference in compositional distribution can be attributed to the inherent properties of the starting precursor and variation in processing conditions. The increase in HTC temperature increases the water density which in turn enhances the rate of hydrolysis of the ether and carbon–carbon bonds of alkylphenol in lignin [84]. According to Amen-Chen et al. [85], the possible mechanism for lignin degradation begins with the elimination of alkyl hydroxyl groups in the alpha position from the propane side-chain along with a beta-ether cleavage to produce monolignols such as p-coumaryl alcohol, coniferyl alcohol and sinapyl alcohol. This is followed by the transfer of hydrogen from the hydroxyl group at gamma-position to free radical species which leads to the formation of methoxy phenols, dimers and formaldehyde. The thermal degradation of initially formed 2-methoxy-phenol at high temperature yielded mainly catechol, phenol, and gaseous products (methane and carbon dioxide). The subsequent hydrolysis of catechol leads to the production of phenol derivatives [30]. It is noted that temperature and reaction time were essential for the formation of phenol from guaiacol.

4. Conclusion

This study has shown that HTC can be used to produce coal-like biofuel from PKL. Amidst all variables, HTC temperature has the most pronounced effect on the biocoal yield and quality, followed by residence time while water to biomass ratio shows no effect on PKL carbonisation except for inorganic metal removal. Despite lower mass yield at a higher temperature, the biocoals produced are characterised by higher carbon content, higher aromaticity, enhanced higher heating value, greater extent of coalification, and satisfactory inorganic metals removal. The optimum conditions for removal of alkaline and alkaline earth metals were HTC temperature of 260 °C, the residence time of 3 h and biomass to water ratio of 1:5. HTC nearly removes all alkaline and alkaline earth metals responsible for slagging, fouling and corrosion under this condition. The process waters contain high concentrations of phenolic compounds. The gaseous phase is composed of mainly CO_2, with some CO and traces of hydrocarbon gases. Consequently, this study has shown that HTC has remarkable potential for converting PKL into low ash coal-like biofuel. Further studies shall investigate the effect of

Table 6
Peak identification of the HTC liquid products of pine Kraft Lignin obtained under different conditions.

	RT (min)	Compound Name	Peak Area (% of ion count)							
			260 °C – 1 h		260 °C – 3 h		280 °C – 1 h		280 °C – 3 h	
			01:03	01:05	01:03	01:05	01:03	01:05	01:03	01:05
1	21.181	Phenol			2					
2	22.113	Phenol, 2-methoxy-(Guaiacol)			9.97					
3	24.265	Phenol, 3-methyl-/M-Cresol			0.32			1.74	1.35	2.67
4	24.372	Phenol, 2-methyl-/O-cresol			0.61				0.44	
5	24.631	Phenol, 2-methoxy-3-methyl-			0.39				0.85	0.62
6	25.641	Phenol, 2-methoxy-4-methyl-/P-cresol			6.54				0.63	0.44
7	27.266	Phenol, 4-ethyl-			0.57					
8	28.481	Phenol, 4-ethyl-2-methoxy			6.89	0.79	0.94	0.77	0.99	1.3
9	31.267	Phenol, 2-methoxy-4-propyl-/Cerulignol	0.48	0.49	4.81	1.1	0.81	1.08	0.73	1.11
10	31.555	Catechol or Pyrocatechol	1.24	2.49	1.71	3.86	5.3	2.42	29.75	23.19
11	32.003	Phenol, 2,6-dimethoxy-/Syringol	1.51	1.16	1.33	2.52	1.85	1.82	2.06	2.68
12	35.014	Vanillin	2.43	9.09	0.81	2.24	2.08	8.06	2.51	1.61
13	37.132	Phenol, 3,4-dimethoxy-	0.46	0.46	0.46	0.5	0.42	0.39	0.39	0.37
14	37.517	Apocynin	12.39	12.83	5.01	11.63	9.37	11.03	5.4	6.71
15	38.913	Vanillyl methyl ketone	19.59	21.18	7.87	18.18	14.64	15	10.45	13
16	39.181	Homovanillyl alcohol	2.14	1.1	0.33	1.99	2.3	1.98	2.57	2.35
17	39.835	1-(2-Hydroxy-4-methoxyphenyl)propan-1-one	0.98	1.19	1.03	1.61	1.23	1.52	1.46	1.49
18	40.303	Butyrovanillone	2.34	2.93	0.86	1.53	2.06	1.89	0.54	0.91
19	41.479	Coniferyl alcohol	0.38	0.44	0.34	0.59	0.8	0.56	0.51	0.6
20	42.031	Butan-2-one, 4-(3-hydroxy-2-methoxyphenyl)-	0.25	0.23	0.34	0.64	0.46	0.52	0.35	0.43
21	42.504	Guaiacol propanaol	43.24	38.78	37.07	35.48	34.91	32.78	34.52	33.43
22	43.724	Benzenemethanol, 3,4,5-trimethoxy-	0.38	0.40	0.41	0.43	0.47	0.41	0.34	0.42
23	58.24	2-Propanone, 1-hydroxy-3-(4-hydroxy-3-methoxyphenyl)-	2.04	0.71	1.71	4.08	1.7	2.5	0.7	0.85
			89.47	92.85	91.38	87.17	79.34	84.47	96.54	93.33

the lignin biocoal on the viscoelastic properties of coking coal to establish its suitability as an additive for coke making.

CRediT authorship contribution statement

Umaru Musa: Conceptualization, Methodology, Formal analysis, Data curation, Validation, Investigation, Funding acquisition, Visualization, Writing – original draft, Writing – review & edit. **Miguel Castro-Díaz:** Supervision, Methodology, Validation, Writing – review & editing. **Clement N. Uguna:** Supervision, Methodology, Validation, Writing – review & editing. **Colin E. Snape:** Conceptualization, Supervision, Project administration, Visualization, Writing – review & editing.

Declaration of Competing Interest

The authors declare that they have no known competing financial interests or personal relationships that could have appeared to influence the work reported in this paper.

Acknowledgement

The authors wish to acknowledge the Nigerian Government for funding Umaru Musa's PhD programme through the Petroleum Technology Development Fund (PTDF) Oversea Scholarship Scheme (OSS) (PTDF/ED/PHD/MU/1155/17).

References

[1] Cabeza LF, Palacios A, Serrano S, Ürge-Vorsatz D, Barreneche C. Comparison of past projections of global and regional primary and final energy consumption with historical data. Renew Sustain Energy Rev 2018;82:681–8.
[2] Janssens-Maenhout G, Crippa M, Guizzardi D, Muntean M, Schaaf E, Olivier JG, et al. Fossil CO2 & GHG emissions of all world countries. Luxembourg: Publications Office of the European Union; 2017.
[3] IEA, World Energy Outlook 2010, Paris (with additional data supplied from IEA). (2010) http://www.iea.org/publications/freepublications/publication/weo2010.pdf.
[4] Metz B, Davidson O, De Coninck HC, Loos M, Meyer L. IPCC special report on carbon dioxide capture and storage, 2005.
[5] Álvarez-Murillo A, Román S, Ledesma B, Sabio E. Study of variables in energy densification of olive stone by hydrothermal carbonization. J Anal Appl Pyrol 2015;113:307–14.
[6] Edenhofer O, Pichs-Madruga R, Sokona Y, Seyboth K, Matschoss P, Kadner S, Zwickel T, Eickemeier P, Hansen G, Schlömer S, von Stechow C. IPCC special report on renewable energy sources and climate change mitigation. Prepared By Working Group III of the Intergovernmental Panel on Climate Change, Cambridge University Press, Cambridge, UK. 2011.
[7] Libra JA, Ro KS, Kammann C, Funke A, Berge ND, Neubauer Y, et al. Hydrothermal carbonization of biomass residuals: a comparative review of the chemistry, processes and applications of wet and dry pyrolysis. Biofuels 2011;2(1):71–106.
[8] Smith AM, Singh S, Ross AB. Fate of inorganic material during hydrothermal carbonisation of biomass: Influence of feedstock on combustion behaviour of hydrochar. Fuel 2016;169:135–45.
[9] Stirling RJ, Snape CE, Meredith W. The impact of hydrothermal carbonisation on the char reactivity of biomass. Fuel Process Technol 2018;1:152–8.
[10] Peterson AA, Vogel F, Lachance RP, Fröling M, Antal Jr MJ, Tester JW. Thermochemical biofuel production in hydrothermal media: a review of sub-and supercritical water technologies. Energy Environ Sci 2008;1(1):32–65.
[11] Liu Z, Quek A, Hoekman SK, Balasubramanian R. Production of solid biochar fuel from waste biomass by hydrothermal carbonization. Fuel 2013;103:943–9.
[12] Funke A, Ziegler F. Hydrothermal carbonization of biomass: a summary and discussion of chemical mechanisms for process engineering. Biofuels Bioprod Bioref 2010;4(2):160–77.
[13] Kambo HS, Dutta A. Comparative evaluation of torrefaction and hydrothermal carbonization of lignocellulosic biomass for the production of solid biofuel. Energy Convers Manage 2015;105:746–55.
[14] Fang J, Zhan L, Ok YS, Gao B. Minireview of potential applications of hydrochar derived from hydrothermal carbonization of biomass. J Ind Eng Chem 2018;57:15–21.
[15] Hu B, Wang K, Wu L, Yu SH, Antonietti M, Titirici MM. Engineering carbon materials from the hydrothermal carbonization process of biomass. Adv Mater 2010;22(7):813–28.
[16] Oliveira I, Blöhse D, Ramke HG. Hydrothermal carbonization of agricultural residues. Bioresour Technol 2013;142:138–46.
[17] Huber GW, Iborra S, Corma A. Synthesis of transportation fuels from biomass: chemistry, catalysts, and engineering. Chem Rev 2006;106(9):4044–98.
[18] Nhuchhen DR, Basu P, Acharya B. A comprehensive review on biomass torrefaction. Int J Renew Energy Biofuels 2014;2014:1–56.
[19] Wong SS, Shu R, Zhang J, Liu H, Yan N. Downstream processing of lignin-derived feedstock into end products. Chem Soc Rev 2020;49(15):5510–60.
[20] Forchheim D, Hornung U, Kruse A, Sutter T. Kinetic modelling of hydrothermal lignin depolymerisation. Waste Biomass Valor 2014;5(6):985–94.
[21] Li T, Takkellapati S. The current and emerging sources of technical lignins and their applications. Biofuels Bioprod Bioref 2018;12(5):756–87.
[22] Barrera-Martínez I, Guzmán N, Peña E, Vázquez T, Cerón-Camacho R, Folch J, et al. Ozonolysis of alkalinene lignin and sugarcane bagasse: Structural changes and their effect on saccharification. Biomass Bioenergy 2016;94:167–72.
[23] Ragauskas AJ, Beckham GT, Biddy MJ, Chandra R, Chen F, Davis MF, et al. Lignin valorization: improving lignin processing in the biorefinery. Science 2014;344(6185):1246843.
[24] Ragauskas EJ, Ragauskas AJ. US–Swedish bridge to the future: sustainable forest biorefining. Biofuels Bioprod Bioref 2014;8(3):295–7.

[25] Luo H, Abu-Omar MM. Chemicals from lignin. Encyclopedia of Sustainable Technologies 2017;3:573–85.
[26] Mandlekar N, Cayla A, Rault F, Giraud S, Salaün F, Malucelli G, et al. An overview on the use of lignin and its derivatives in fire retardant polymer systems. Lignin-Trends Appl 2018;9:207–31.
[27] Bajwa DS, Pourhashem G, Ullah AH, Bajwa SG. A concise review of current lignin production, applications, products and their environmental impact. Ind Crops Prod. 2019; 139:111526.
[28] Wikberg H, Ohra-aho T, Pileidis F, Titirici MM. Structural and morphological changes in Kraft lignin during hydrothermal carbonization. ACS Sustainable Chem Eng 2015;3(11):2737–45.
[29] Gollakota AR, Kishore N, Gu S. A review on hydrothermal liquefaction of biomass. Renew Sustain Energy Rev 2018;81:1378–92.
[30] Karagöz S, Bhaskar T, Muto A, Sakata Y. Comparative studies of oil compositions produced from sawdust, rice husk, lignin and cellulose by hydrothermal treatment. Fuel 2005;84(7–8):875–84.
[31] Kang S, Li X, Fan J, Chang J. Hydrothermal conversion of lignin: A review. Renew Sustain Energy Rev 2013;27:546–58.
[32] Ye Y, Fan J, Chang J. Effect of reaction conditions on hydrothermal degradation of cornstalk lignin. J Anal Appl Pyrol 2012;94:190–5.
[33] Liu C, Wu S, Zhang H, Xiao R. Catalytic oxidation of lignin to valuable biomass-based platform Chemicals: A review. Fuel Process Technol 2019;191:181–201.
[34] Belkheiri T, Andersson S-I, Mattsson C, Olausson L, Theliander H, Vamling L. Hydrothermal Liquefaction of Kraft lignin in sub-critical water: the influence of the sodium and potassium fraction. Biomass Convers Biorefin 2018;8(3):585–95.
[35] Hu J, Shen D, Wu S, Zhang H, Xiao R. Effect of temperature on structure evolution in char from hydrothermal degradation of lignin. J Anal Appl Pyrol 2014;106:118–24.
[36] Lu X, Berge ND. Influence of feedstock chemical composition on product formation and characteristics derived from the hydrothermal carbonization of mixed feedstocks. Bioresour Technol 2014;166:120–31.
[37] Seehra MS, Pyapalli SK, Poston J, Atta-Obeng E, Dawson-Andoh B. Hydrothermal conversion of commercial lignin to carbonaceous materials. J Indian Acad Wood Sci 2015;12(1):29–36.
[38] Dinjus E, Kruse A, Troeger N. Hydrothermal carbonization: 1. Influence of lignin in lignocelluloses.Chemie Ingenieur Technik. 2011; 83(10):1734-41.
[39] Kim D, Lee K, Park KY. Upgrading the characteristics of biochar from cellulose, lignin, and xylan for solid biofuel production from biomass by hydrothermal carbonization. Ind Eng Chem 2016;42:95–100.
[40] Correa CR, Hehr T, Rauscher Y, Alhnidi MJ, Kruse A. Biomass Carbonization-An experimental comparison between pyrolysis and hydrothermal carbonization. J Anal Appl Pyrol 2019;140:137–47.
[41] Sangchoom W, Mokaya R. Valorization of lignin waste: carbons from hydrothermal carbonization of renewable lignin as superior sorbents for CO2 and hydrogen storage. ACS Sustain Chem Eng 2015;3(7):1658–67.
[42] Atta-Obeng E, Dawson-Andoh B, Seehra MS, Geddam U, Poston J, Leisen J. Physico-chemical characterization of carbons produced from technical lignin by sub-critical hydrothermal carbonization. Biomass Bioenergy 2017;107:172–81.
[43] Volpe M, Goldfarb JL, Fiori L. Hydrothermal carbonization of Opuntia ficus-indica cladodes: Role of process parameters on hydrochar properties. Bioresour Technol 2018;247:310–8.
[44] Koppejan J, Van Loo S. The handbook of biomass combustion and co-firing. Routledge; 2012.
[45] Smith AM, Whittaker C, Shield I, Ross AB. The potential for production of high-quality bio-coal From early harvested Miscanthus by hydrothermal carbonisation. Fuel 2018;220:546–57.
[46] Reza MT, Lynam JG, Uddin MH, Coronella CJ. Hydrothermal carbonization: Fate of inorganics. Biomass Bioenergy 2013;49:86–94.
[47] Yao Z, Ma X. Effects of hydrothermal treatment on the pyrolysis behavior of Chinese fan palm. Bioresour Technol 2018;247:504–12.
[48] Novianti S, Nurdiawati A, Zaini IN, Prawisudha P, Sumida H, Yoshikawa K. Low-potassium fuel production from empty fruit bunches by hydrothermal treatment processing and water leaching. Energy Procedia 2015;75:584–9.
[49] Smith AM, Ross AB. The influence of residence time during hydrothermal carbonisation of miscanthus on bio-coal combustion chemistry. Energies 2019;3:523.
[50] Su H, Zhou X, Zheng R, Zhou Z, Zhang Y, Zhu G, Yu C, Hantoko D, Yan M. Hydrothermal carbonization of food waste after oil extraction pre-treatment: Study on hydrochar fuel characteristics, combustion behavior, and removal behavior of sodium and potassium. Sci Total Environ. 2021; 754:142192.
[51] Channiwala SA, Parikh PP. A unified correlation for estimating HHV of solid, liquid and gaseous fuels. Fuel. 2002; 81(8):1051-63.
[52] Kang S, Li X, Fan J, Chang J. Characterization of hydrochars produced by hydrothermal carbonization of lignin, cellulose, D-xylose, and wood meal. Ind Eng Chem Res 2012;51(26):9023–31.
[53] Hoekman SK, Broch A, Robbins C. Hydrothermal carbonization (HTC) of lignocellulosic biomass. Energy Fuels 2011;25(4):1802–10.
[54] Lisperguer J, Perez P, Urizar S. Structure and thermal properties of lignins: characterization by Infrared spectroscopy and differential scanning calorimetry. J Chilean Chem Soc 2009;54(4):460–3.
[55] Pahla G, Mamvura TA, Ntuli F, Muzenda E. Energy densification of animal waste lignocelluloses biomass and raw biomass. S Afr J Chem Eng 2017;24(1):168–75.
[56] Svensson S. Minimizing the sulphur content in Kraft lignin. (2008). Degree project University of Stockholm, accessed on 30 March from https://www.diva-portal.org/smash/get/diva2%3A1676/FULLTEXT01.pdf.
[57] Khan TA, Saud AS, Jamari SS, Ab Rahim MH, Park JW, Kim HJ. Hydrothermal carbonization of lignocellulosic biomass for carbon rich material preparation: A review. Biomass Bioenergy. 2019; 130:105384.
[58] Castro-Díaz M, Vega MF, Díaz-Faes E, Barriocanal C, Musa U, Snape C. Evaluation of demineralized lignin and lignin-phenolic resin blends to produce biocoke suitable for blast furnaceoperation. Fuel. 2019; 258:116125.
[59] Durie RA, editor. The science of Victorian brown coal: structure, properties and consequences for utilization. Butterworth-Heinemann; 2013.
[60] Kokonya S, Castro-Díaz M, Barriocanal C, Snape CE. An investigation into the effect of fast heating on fluidity development and coke quality for blends of coal and biomass. Biomass Bioenergy 2013;56:295–306.
[61] MacPhee JA, Gransden JF, Giroux L, Price JT. Possible CO2 mitigation via addition of charcoal to coking coal blends. Fuel Process Technol 2009;90(1):16–20.
[62] Suopajärvi H, Dahl E, Kemppainen A, Gornostayev S, Koskela A, Fabritius T. Effect of charcoal and Kraft-lignin addition on coke compression strength and reactivity. Energies 2017;11:1850.
[63] Nizamuddin S, Baloch HA, Griffin GJ, Mubarak NM, Bhutto AW, Abro R, et al. An Overview of effect of process parameters on hydrothermal carbonization of biomass. Renew Sustain Energy Rev 2017;73:1289–99.
[64] Van Krevelen DW. Coal: Typology-physics-chemistry-constitution. Elsevier; 1993.
[65] Aliyu M, Iwabuchi K, Itoh T. Upgrading the fuel properties of hydrochar by co-hydrothermal carbonisation of dairy manure and Japanese larch (Larix kaempferi): product characterisation, thermal behaviour, kinetics and thermodynamic properties. Biomass Convers Biorefin 2021;28:1–6.
[66] Lin H, Zhang L, Zhang S, Li Q, Hu X. Hydrothermal carbonization of cellulose in aqueous phase of bio-oil: The significant impacts on properties of hydrochar. Fuel. 2022;315:123132.
[67] Leng L, Huang H, Li H, Li J, Zhou W. Biochar stability assessment methods: a review. Sci Total Environ. 2019; 647:210-22.
[68] Donar YO, Çağlar E, Sınağ A. Preparation and characterization of agricultural waste biomass based hydrochars. Fuel 2016;183:366–72.
[69] Peters KE, Xia X, Pomerantz AE, Mullins OC. Geochemistry applied to evaluation of unconventional resources. In Unconventional oil and gas resources handbook 2016 (pp. 71-126). Gulf Professional Publishing.
[70] Gamgoum R, Dutta A, Santos RM, Chiang YW. Hydrothermal conversion of neutral sulfite semi- chemical red liquor into hydrochar. Energies 2016;6:435.
[71] Gao Y, Wang X, Wang J, Li X, Cheng J, Yang H, et al. Effect of residence time on chemical and structural properties of hydrochar obtained by hydrothermal carbonization of water hyacinth. Energy 2013;58:376–83.
[72] Saddawi A, Jones JM, Williams A, Le Coeur C. Commodity fuels from biomass through pretreatment and torrefaction: effects of mineral content on torrefied fuel characteristics and quality. Energy Fuels 2012;26(11):6466–74.
[73] Chen J, Chen Z, Wang C, Li X. Calcium-assisted hydrothermal carbonization of an alginate for the production of carbon microspheres with unique surface nanopores. Mater Lett 2012;67(1):365–8.
[74] Wang L, Chang Y, Li A. Hydrothermal carbonization for energy-efficient processing of sewage sludge: A review. Renew Sustain Energy Rev 2019;108:423–40.
[75] Wang L, Chang Y, Liu Q. Fate and distribution of nutrients and heavy metals during hydrothermal carbonization of sewage sludge with implication to land application. J Cleaner Prod 2019;225:972–83.
[76] Sharma RK, Wooten JB, Baliga VL, Lin X, Chan WG, Hajaligol MR. Characterization of chars from pyrolysis of lignin. Fuel 2004;83(11–12):1469–82.
[77] Hatcher PG. Chemical structural studies of natural lignin by dipolar dephasing solid-state ^{13}C nuclear magnetic resonance. Org Geochem 1987;11(1):31–9.
[78] Kline LM, Hayes DG, Womac AR, Labbé N. Simplified determination of lignin content in hard and soft woods via UV-spectrophotometric analysis of biomass dissolved in ionic liquids. Bioresources 2010;5(3):1366–83.
[79] Falco C, Baccile N, Titirici MM. Morphological and sstructural differences between glucose, cellulose and lignocellulosic biomass derived hydrothermal carbons. Green Chem 2011;13(11):3273–81.
[80] Das B, Suresh A, Dash PS, Chandra S, Diaz MC, Stevens LA, et al. Understanding the unusual fluidity characteristics of high ash Indian bituminous coals. Fuel Process Technol 2018;176:258–66.
[81] Odeh AO. Comparative study of the aromaticity of the coal structure during the char formation process under both conventional and advanced analytical techniques. Energy Fuels 2015;29(4):2676–84.
[82] Takada D, Ehara K, Saka S. Gas chromatographic and mass spectrometric (GC-MS) analysis of Lignin-derived products from Cryptomeria japonica treated in supercritical water. J Wood Sci 2004;50(3):253–9.
[83] Du L, Wang Z, Li S, Song W, Lin W. A comparison of monomeric phenols produced from lignin by fast pyrolysis and hydrothermal conversions. Int J Chem Reactor Eng 2013;11(1):135–45.
[84] Wahyudiono, Sasaki M, Goto M. Recovery of phenolic compounds through the decomposition of lignin in near and supercritical water. Chem Eng Process: Process Intens 2008;47(9-10):1609–19.
[85] Amen-Chen C, Pakdel H, Roy C. Production of monomeric phenols by thermochemical conversion of biomass: a review. Bioresour Technol 2001;79(3):277–99.